ORIGINAL ARTICLE

Cancer Science WILEY

Ki67 expression and localization of T cells after neoadjuvant therapies as reliable predictive markers in rectal cancer

Ken Imaizumi[1,2,3] 🆔 | Toshihiro Suzuki[2] 🆔 | Motohiro Kojima[4] 🆔 |
Manami Shimomura[2] | Naoki Sakuyama[1] 🆔 | Yuichiro Tsukada[1] | Takeshi Sasaki[1] |
Yuji Nishizawa[1] | Akinobu Taketomi[3] | Masaaki Ito[1] | Tetsuya Nakatsura[2] 🆔

[1]Deparment of Colorectal Surgery, National Cancer Center Hospital East, Kashiwa, Japan

[2]Division of Cancer Immunotherapy, Exploratory Oncology Research & Clinical Trial Center, National Cancer Center, Kashiwa, Japan

[3]Department of Gastroenterological Surgery I, Graduate School of Medicine, Hokkaido University, Sapporo, Japan

[4]Division of Pathology, National Cancer Center Hospital East, Kashiwa, Japan

Correspondence
Tetsuya Nakatsura, Division of Cancer Immunotherapy, Exploratory Oncology Research & Clinical Trial Center, National Cancer Center, Kashiwa, Japan.
Email: tnakatsu@east.ncc.go.jp

Funding information
National Cancer Center Research and Development Fund, Grant/Award Number: 25-A-7 and 28-A-8

Abstract

Chemoradiotherapy (CRT) is the standard neoadjuvant therapy for locally advanced rectal cancer (RC). However, neoadjuvant chemotherapy (NAC) also shows favorable outcomes. Although the immunological environment of RC has been thoroughly discussed, the effect of NAC on it is less clear. Here, we investigated the immunological microenvironment, including T cell infiltration, activation, and topological distribution, of resected RC tissue after neoadjuvant therapies and evaluated the correlation between T cell subsets and patient prognosis. Rectal cancer patients (n = 188) were enrolled and categorized into 3 groups, namely CRT (n = 41), NAC (n = 46), and control (surgery alone; n = 101) groups. Characterization of residual carcinoma cells and T cell subsets in resected tissues was performed using multiplex fluorescence immunohistochemistry. The densities of total and activated (Ki67^{high}) T cells in tissues after NAC, but not CRT, were higher than in control. In both CRT and NAC groups, patients presenting with higher treatment effects showed aggressive infiltration of T cell subsets into carcinomas. Multivariate analyses of pathological and immunological features and prognosis revealed that carcinoma Ki67^{high}CD4$^+$ T cells after CRT and stromal Ki67^{high}CD8$^+$ T cells after NAC are important prognostic factors, respectively. Our results suggest that evaluation of T cell activation with Ki67 expression and its tumor localization can be used to determine the prognosis of advanced RC after neoadjuvant therapies.

KEYWORDS
multiplexed fluorescent immunohistochemistry, neoadjuvant chemoradiotherapy, neoadjuvant chemotherapy, rectal cancer, tumor-infiltrating lymphocyte

1 | INTRODUCTION

The current standard treatment for locally advanced rectal cancer (RC) is preoperative chemoradiotherapy (CRT). Although CRT is known to improve local control of the tumor, it is also reported to cause postoperative complications and pelvic dysfunction.[1-4] To maintain the function of pelvic nerves and muscles, neoadjuvant chemotherapy (NAC) was recently established.[5,6] Tailored treatments, in which choosing or combining CRT and NAC is made on a case-by-case basis, will be significant in the future.[7]

It has been reported that tumor-infiltrating lymphocytes (TILs) determine not only antitumor surveillance but also the treatment efficacy of neoadjuvant therapy.[8,9] Tumor-infiltrating lymphocytes positively control tumor immunity and their marked infiltration was reported to be associated with better clinical outcomes in various cancers.[10-13] High accumulation of intratumoral CD8$^+$ T cells shows favorable prognosis in RC patients with or without preoperative CRT.[14,15] However, no study has evaluated the immunological environment of RC after NAC. Evaluating changes in the immunological environment after neoadjuvant therapies could reveal immune cell components associated with treatment efficacy and patient prognosis. Currently, combination studies with immunological checkpoint inhibitors, chemotherapy, radiotherapy, and CRT are underway for various tumors to enhance the antitumor immune response.[7,16,17] Although some clinical trials revealed that immunological check point inhibitors, such as mAbs against programmed cell death-1, are effective against various cancers,[16-18] most advanced colorectal cancers, excluding high microsatellite instability colorectal cancer, are insensitive to immunological checkpoint inhibitors.[19] Thus, assessing the immunological environment and its effect on antitumor immune response after neoadjuvant therapies could provide a proof of concept for the benefits of immune checkpoint inhibitors in combination with CRT and NAC for advanced RC treatment.

Recently, multiplex fluorescence immunohistochemistry (mFIHC) has emerged as an effective tool for comprehensive analysis of immune cell type in the tumor microenvironment.[20-22] Previously, studies evaluated stromal or intratumoral lymphocytes in addition to analyzing TIL subsets and have reported that TIL localization in the epithelial compartment of tumors is important because nonspecific infiltration of lymphocytes into the tumor stroma is often observed after treatment.[23,24] The nuclear protein Ki67 is commonly used to assess cell proliferation and measure the proliferative capacity of tumor cells and T cells. Ki67 expression is observed during all active phases of cell division but not during DNA repair or the cell quiescent phase.[25] For some chronic diseases, such as HIV infection, cancer, and autoimmune diseases, the Ki67 expression pattern in T cells is used to evaluate antigen-specific T cell expansion.[26,27]

In this study, using mFIHC analysis by staining with opal fluorescence molecules and multispectra imaging, we analyzed the tumor microenvironment and immunological features of RC, including T cell activation by Ki67 expression, and elucidated the histological alterations mediated by NAC and CRT compared with surgery alone. Moreover, we evaluated the correlation between TIL subsets and recurrence-free survival (RFS) to find novel prognostic markers after neoadjuvant therapies.

2 | MATERIALS AND METHODS

2.1 | Patient cohort

Ninety-nine locally advanced RC patients (T3 or T4, N0 or T any, N1-2) who had received preoperative therapy between January 2001 and June 2014 at the National Cancer Center Hospital East (NCCHE, Chiba, Japan) were recruited. Of these, 48 and 51 cases received preoperative CRT and NAC, respectively. The CRT group received preoperative fluoropyrimidine-based chemotherapy (infused 5-fluorouracil or oral capecitabine) and fractionated radiation (total 45 Gy in 25 fractions or total 50.4 Gy in 28 fractions). Surgical resection was performed 4-12 weeks after CRT. The NAC group received 3-8 courses of preoperative FOLFOX, followed by surgery 4-8 weeks after NAC. Seven patients in the CRT group and 5 patients in the NAC group achieved pathological complete response (pCR). These 12 cases with pCR were excluded because of no detectable cancer tissue in the resected specimens. As control subjects, 101 patients who underwent surgery alone were recruited. Finally, 188 patients with locally advanced RC were enrolled and categorized into 3 groups according to pretreatment: CRT group (n = 41), NAC group (n = 46), and control group (n = 101). The study conformed to the ethical guidelines of the 1975 Declaration of Helsinki and was approved by the institutional review board of NCCHE (protocol no. 2016-157).

2.2 | Histopathology

Preoperative clinical staging and pathological staging were carried out according to the UICC classification (7th edition). The local treatment effect was evaluated by tumor regression grade (TRG) according to the method described by the American Joint Committee on Cancer and the College of American Pathologists.[28,29] Other variables obtained from the pathology report were pathological stage (pStage and ypStage), lymphatic invasion (LYI), vascular invasion (VI), and perineural invasion (PNI).

2.3 | Construction of 4-point tissue microarrays

Formalin-fixed, paraffin-embedded tumor blocks and corresponding slides stained with H&E from the 188 cases were collected from the institutional pathology archive. For tissue microarray (TMA), a gastrointestinal pathologist selected 2 target areas from the center of the tumor and the invasive margin, after which a total of 4 tumor cores per case were picked up using a punch tip (φ 2 mm; Azumaya) (Figure S1A,B).[30,31] One TMA block contained 48 tissue cores; in total, 16 TMA sets consisting of 768 core specimens were prepared for this study.

2.4 | Immunohistochemistry for mismatch repair status

To identify mismatch repair (MMR) status, we performed conventional immunohistochemistry (IHC) using MLH1 (1:500; BD Pharmingen), MSH2 (1:50; Calbiochem), MSH6 (1:1000; BD Pharmingen), and PMS2 (1:50; Dako, Santa Clara, CA) Abs. Immunohistochemistry was carried out on 4-μm thick sections obtained from the TMA block (Figure S1C). Tumor cell nuclei that did not display any brown staining for the abovementioned markers were considered MMR deficient (dMMR).

2.5 | Multiplex fluorescence IHC and image analysis

Tissue sections (4-μm thick) obtained from TMA blocks were subjected to mFIHC staining using the PerkinElmer Opal Kit (PerkinElmer). The Abs, dilutions, and activation conditions used are listed in Table S1. Images were captured using an automated multisector imaging system (Vectra version 3.0; PerkinElmer). An image analysis program (Inform; PerkinElmer) was used to segment tumor tissues into carcinoma and stromal areas and to detect immune cells with specific phenotypes, after which the distribution of immune cells was analyzed (Figure S2). Training sessions for tissue segmentation and phenotype recognition were carried out repeatedly until the algorithm reached the level of confidence recommended by the program supplier (at least 90% accuracy) before performing the final evaluation.[24,32] After phenotyping typical CD4$^+$ and CD8$^+$ cells using Inform software, gated CD3$^+$ populations by mean fluorescence intensity of CD3, CD3$^+$CD4$^+$, and CD3$^+$CD8$^+$ cells were determined as CD4$^+$ T cells and CD8$^+$ T cells, respectively. A similar gating strategy was used for the analysis of Ki67^{high} population in cytokeratin positive (CK$^+$) cells, CD4$^+$ T cells, and CD8$^+$ T cells using an analytical program (Spotfire version 7.8; TIBCO Software; Figure S3). The area of each tissue category, carcinoma and stroma, was evaluated to assess the density of lymphocytes, represented by (number of lymphocytes) / (pixel area) in each tumor core; an average value of 4 tumor cores was determined. T cells in the carcinoma and stromal areas were defined as carcinoma T cells and stromal T cells, respectively. The ratio of carcinoma to stromal T cells (carcinoma / stromal ratio) was calculated using the ratio of the density of carcinoma T cells to that of stromal T cells.

2.6 | Statistical analysis

Densities of the lymphocyte subsets were represented using box plots with median values and interquartile ranges. The boxplot whiskers indicate the 10th and 90th percentile values. Bar charts show mean values of proportion and ratios of each population.

TABLE 1 Characteristics of patients with rectal cancer

Characteristic	CRT (n = 41)	NAC (n = 46)	Control (surgery alone) (n = 101)	P value CRT vs NAC	P value CRT vs Cont.	P value NAC vs Cont.
Age (years), median (range)	57 (27-77)	57 (27-72)	61 (33-80)	.739	.340	.053
Sex, n (%)						
Male	30 (73.2)	33 (71.7)	66 (65.3)	1.000	1.000	1.000
Female	11 (26.8)	13 (28.3)	35 (34.7)			
Distance from anal verge (cm), median (range)	3.0 (0-6.0)	3.5 (0-6.0)	4.0 (0-6.0)	.266	.116	.996
Clinical TNM stage, n (%)						
II	18 (43.9)	18 (39.1)	54 (53.5)	1.000	1.000	0.450
III	23 (56.1)	28 (60.9)	47 (46.5)			
Pathological TNM stage, n (%)						
I	10 (24.4)	13 (28.3)	22 (21.8)	1.000	1.000	1.000
II	14 (34.1)	12 (26.1)	35 (34.7)			
III	17 (41.5)	21 (45.6)	44 (43.5)			
Lymphatic invasion, n (%)	10 (24.4)	22 (47.8)	53 (52.5)	.124	.012	1.000
Vascular invasion, n (%)	24 (58.5)	21 (45.7)	82 (81.2)	.973	.028	<.001
Perineural invasion, n (%)	14 (34.1)	12 (26.1)	43 (42.6)	1.000	1.000	.250
Tumor regression grade, n (%)						
1	17 (41.5)	13 (28.3)	—	<.001		
2	24 (58.5)	20 (43.5)	—			
3	0 (0)	13 (28.3)	—			
dMMR, n (%)	3 (7.3)	2 (4.3)	6 (5.9)	1.000	1.000	1.000

Abbreviations: —, not applicable; Cont., Control; CRT, chemoradiotherapy; dMMR, deficient mismatch repair; NAC, neoadjuvant chemotherapy.

Error bars on graphs show SDs. Statistical significance was calculated using Dunnett's test and Tukey's test for parametric analysis or the Steel test and Steel–Dwass test for nonparametric analysis. The χ^2 test or Fisher's exact test were used to examine categorical variables. Recurrence-free survival was estimated using the Kaplan-Meier method, and differences in curves between experimental groups were evaluated by the log-rank test. Univariate and multivariate comparisons between various variables, including T cell subsets and RFS, were perfomed using the Cox proportional hazards regression model. Variables with *P* values less than .05 in univariate analysis were included in the multivariable Cox regression model. *P* values less than .05 were considered statistically significant.

All statistical analyses and graphing were performed using EZR version 2.2-5 (Saitama Medical Center, Jichi Medical University), a modified version of R commander, and is designed to add statistical functions frequently used in biostatistics.[33] A graphical user interface for R version 3.3.1 (R Foundation for Statistical Computing) was also used for analysis. Figures were prepared using Autodesk Graphic version 3.0.1 (Autodesk, Inc.).

3 | RESULTS

3.1 | Patient characteristics and RFS after neoadjuvant therapies

Patient characteristics and clinicopathological features are listed in Table 1. There were no significant differences in age, sex, distance from anal verge, clinical TNM stage, pathological TNM stage, or PNI between the 3 groups. Lymphatic invasion was observed less frequently in the CRT group than in the control group. Vascular invasion was also found less frequently in the CRT and NAC groups than in the control group. Tumor regression grade in the CRT group was better than in the NAC group. Eleven patients (5.9%) were dMMR, of which 3 patients (7.3%) were in the CRT group, 2 (4.3%) in the NAC group, and 6 (5.9%) in the control group. There were no significant differences in RFS based on neoadjuvant therapies (3-year RFS, CRT 60.6% vs NAC 63.0%; *P* = .976).

3.2 | Changes in histology and growth activity of residual carcinoma cells after neoadjuvant therapies

Using mFIHC analysis of tumor sections with nuclei, CK, and Ki67 staining, we compared the treatment effects of CRT and NAC based on residual carcinoma areas and their growth activity (Figure 1A). Calculation of the total carcinoma area by Inform software was highly correlated with TRG (Figure 1B). Interestingly, within the same TRG, the individual regions of residual carcinomas in the CRT group (Figure 1A, center panel) tended to be smaller than those in the NAC group (Figure 1A, right panel), although the total residual carcinoma area was comparable between them (Figure 1B). Patients who received CRT had smaller carcinoma masses (<0.01 mm²) than those who received NAC and had the same TRG (Figure 1C). To examine the inhibition of residual carcinoma growth by each neoadjuvant therapy, we evaluated Ki67 expression in CK$^+$ cells and found that the growth activity of CK$^+$ cells was significantly inhibited by CRT, but not by NAC (Figure 1D). Moreover, the proportion of Ki67^{high} in CK$^+$ cells was not altered by the local treatment effects of either CRT or NAC (Figure 1E).

3.3 | Analysis of T cells and their localization in tumor tissue after neoadjuvant therapies

Representative features of CD3/CD4 and CD3/CD8 double staining for surgery alone, CRT, and NAC specimens are shown in Figure 2A, B. Compared with the control group, the densities of carcinoma CD4$^+$ T cells, carcinoma CD8$^+$ T cells, and stromal CD8$^+$ T cells were significantly increased after NAC. In the CRT group, the densities of carcinoma CD4$^+$ T cells and CD8$^+$ T cells were preserved compared with those in the control group, whereas the densities of stromal CD4$^+$ T cells and CD8$^+$ T cells were significantly reduced (Figure 2C, D). After CRT, the carcinoma / stromal ratio of both CD4$^+$ and CD8$^+$ T cells was significantly higher than in the control group, whereas after NAC, only CD8$^+$ T cells tended to infiltrate the carcinoma area (Figure 2E).

## 3.4 | Analysis of the Ki67^{high} subpopulation of T cells after neoadjuvant therapies

Next, we assessed the population of Ki67^{high} T cells in each tissue area to assess T cell activity. Representative images of Ki67 staining in CD4$^+$ and CD8$^+$ T cells are shown in Figure 3A, B, respectively. Similar to total T cells, the densities of carcinoma and stromal Ki67^{high}CD4$^+$ T cells in the NAC group were significantly increased compared with the control group. The density of carcinoma Ki67^{high}CD8$^+$ T cells after NAC also tended to increase.

FIGURE 1 Evaluation of residual rectal carcinoma after neoadjuvant therapies. A, Representative multiplex fluorescence images of the residual carcinoma. Nuclei, cytokeratin (CK), and Ki67 in cells are shown in blue, orange, and white, respectively. B, Total residual carcinoma area after neoadjuvant therapies was quantified using Inform software. *P* values were analyzed by Steel-Dwass test. C, Sizes of individual carcinoma glands in patients after neoadjuvant therapies. According to the mean size of each carcinoma area, patients were sorted into 3 groups: small (pink, <0.01 mm²), medium (yellow, ≥0.01 mm² and <0.02 mm²), and large (green, ≥0.02 mm²). The percentages of patients in these categorizes are shown in the graph. *P* values were analyzed by Fisher's exact test. D, E, Growth activity of residual carcinomas after neoadjuvant therapies (D). Correlation between residual carcinoma growth and tumor regression grade (TRG) after neoadjuvant therapies (E). Growth activity was evaluated by the percentage of Ki67^{high} in CK$^+$ (carcinoma) cells. *P* values were analyzed by Dunnett's test (D) and Tukey's test (E). Cont., control; CRT, chemoradiotherapy; NAC, neoadjuvant chemotherapy

Moreover, the proportion of Ki67^{high}CD4$^+$ T cells after NAC increased, whereas that of Ki67^{high}CD8$^+$ T cells did not change compared with that of the control group. Regarding the CRT group, the densities of stromal Ki67^{high}CD4$^+$ T cells as well as carcinoma and stromal Ki67^{high}CD8$^+$ T cells were significantly decreased compared with that of the control group; however, the proportions of
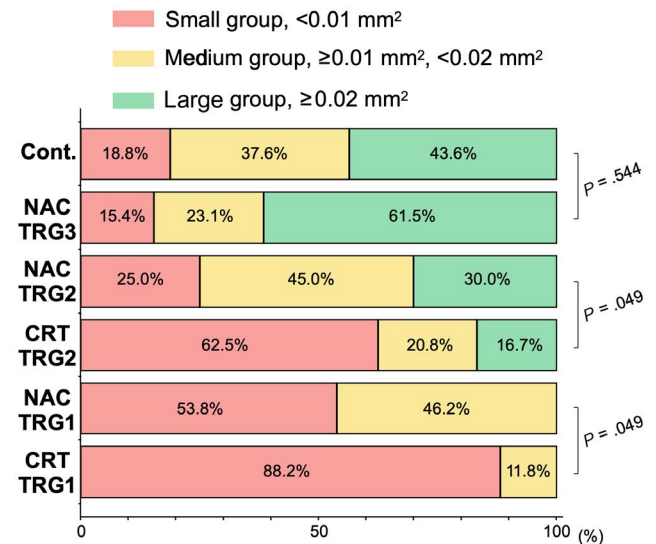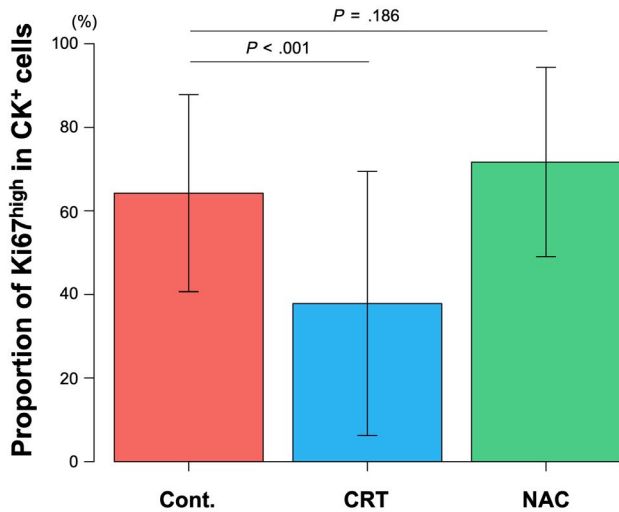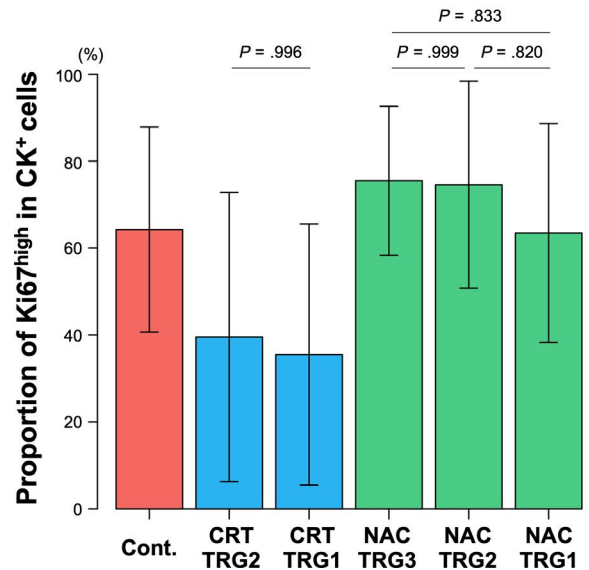
(A)

Blue = nuclei   Orange = cytokeratin   White = Ki67
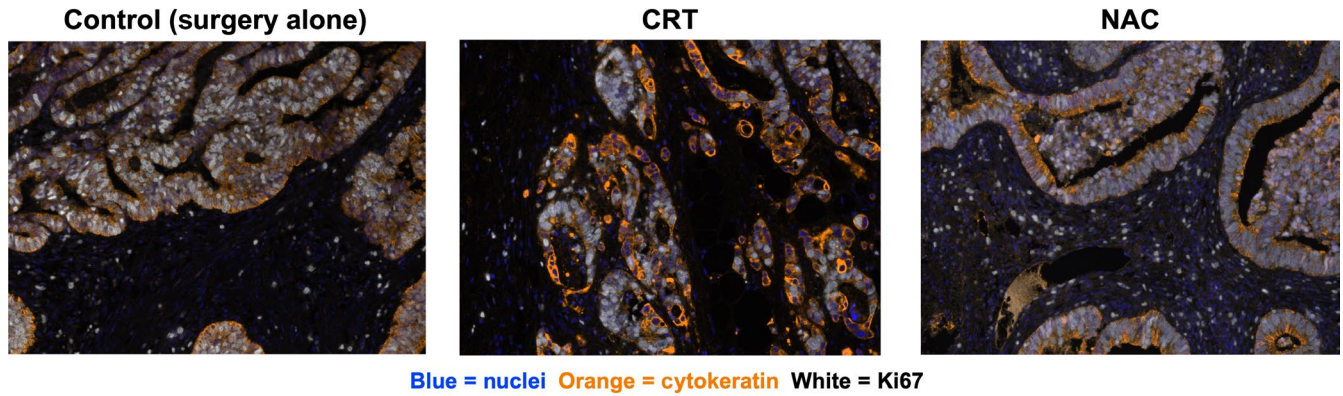
(B)
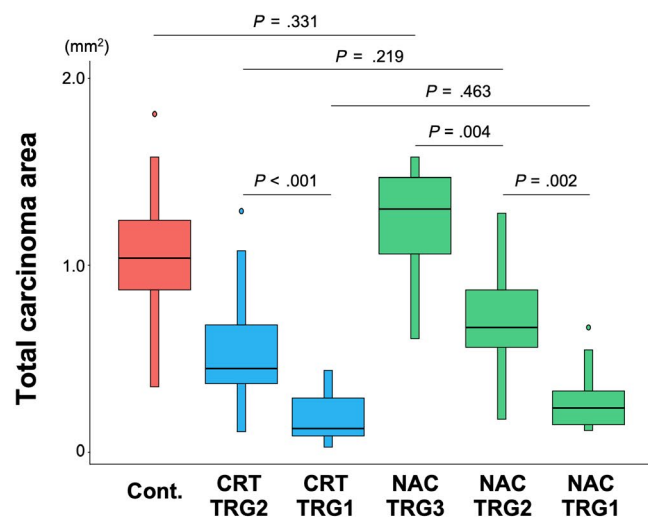
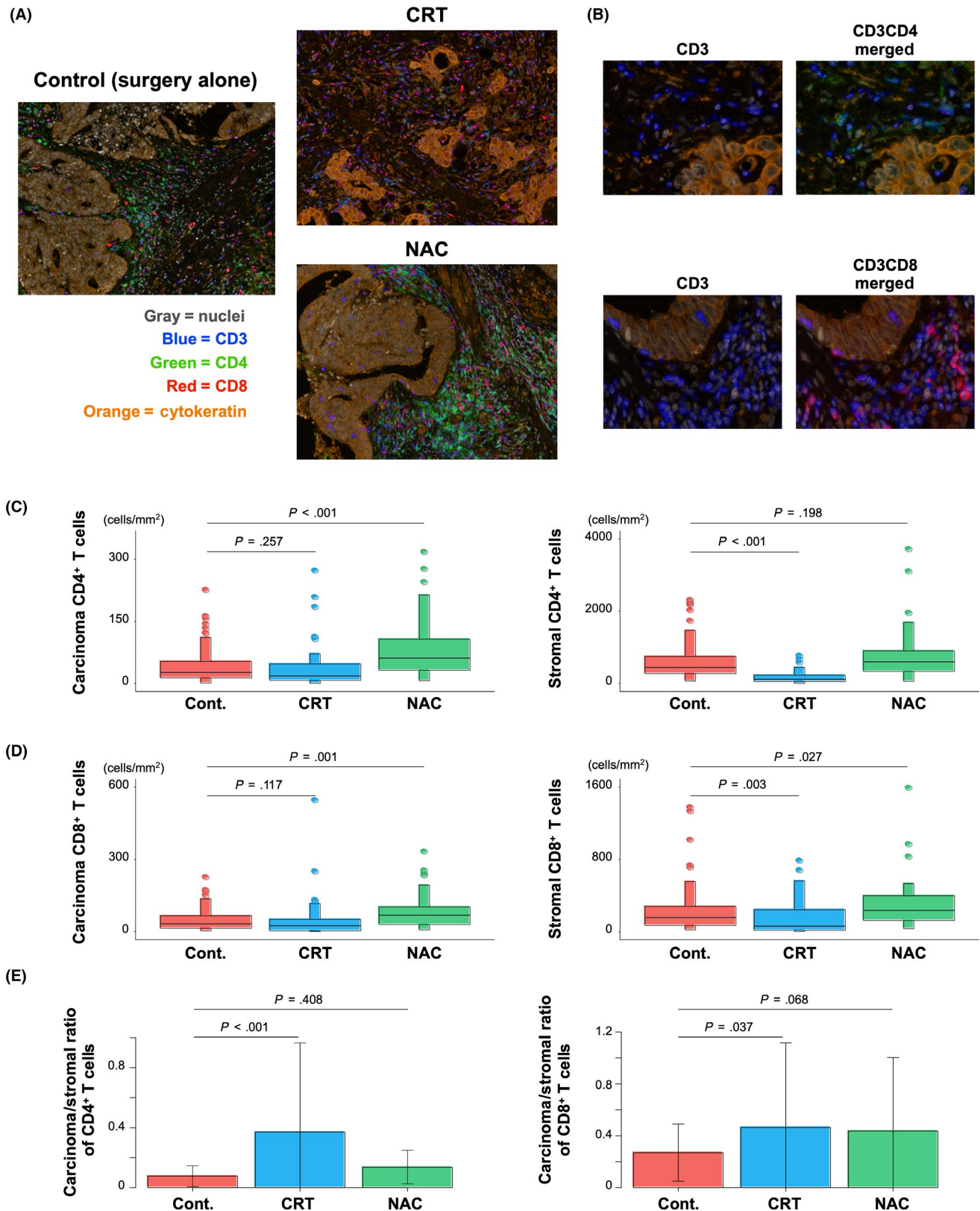**(C)** Carcinoma region size

(D)

(E)

FIGURE 2 Evaluation of tumor-infiltrating T cells after neoadjuvant therapies for rectal cancer. A, Representative multiplex fluorescence images of tumor-infiltrating T cells after neoadjuvant therapies. Nuclei, CD3, CD4, CD8, and cytokeratin in cells are shown in gray, blue, green, red, and orange, respectively. B, Enlarged fluorescence images show CD3$^+$CD4$^+$ cells as CD4$^+$ T cells (upper panels) and CD3$^+$CD8$^+$ cells as CD8$^+$ T cells (lower panels). C, D, Carcinoma (left graph) and stromal (right graph) CD4$^+$ T cell (C) and CD8$^+$ T cell (D) density. P values were analyzed by the Steel test. E, Ratio of carcinoma to stromal CD4$^+$ T cells (left graph) and CD8$^+$ T cells (right graph). P values were analyzed by Dunnett's test. Cont., control; CRT, chemoradiotherapy; NAC, neoadjuvant chemotherapy
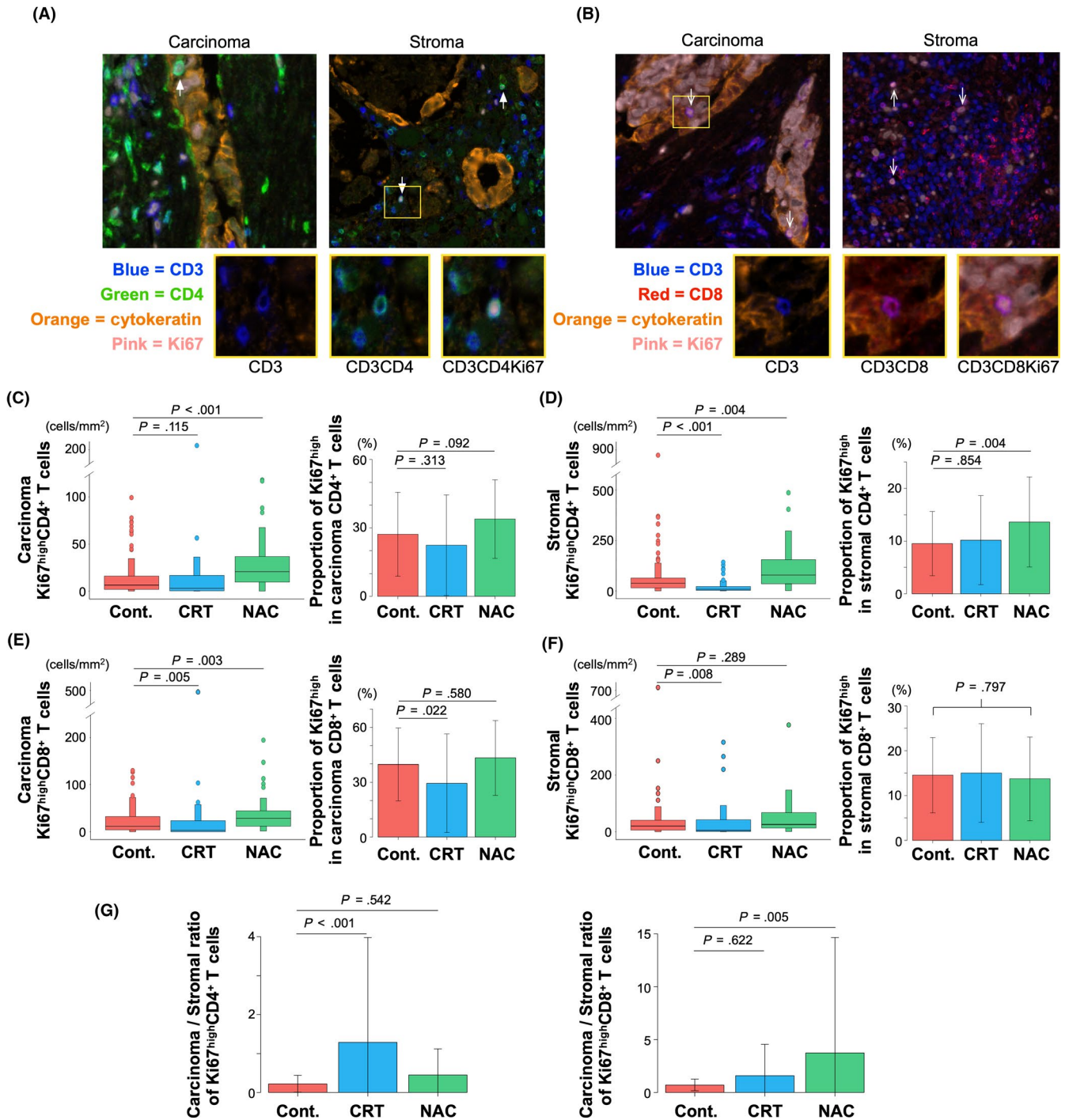
FIGURE 3 Evaluation of Ki67^{high} T cells after neoadjuvant therapies for rectal cancer. A, B, Representative images of Ki67^{high}CD4^{+} T cells (A) and Ki67^{high}CD8^{+} T cells (B). Ki67^{high} subpopulation of T cells was determined by visualizing nuclear Ki67 (pink) expression in each subset. CD4^{+} or CD8^{+} T cells were detected by visualizing CD3 (blue) and CD4 (green) double-positive or CD3 (blue) and CD8 (red) double-positive cells, respectively. White bold arrows indicate CD3^{+}CD4^{+}Ki67^{high} cells (A). White thin arrows indicate CD3^{+}CD8^{+}Ki67^{high} cells (B). Lower photographs show enlarged fluorescence images of the yellow squares in the upper photographs. C–F, Densities (left graph) and proportions (right graph) of carcinoma Ki67^{high}CD4^{+} T cells (C), stromal Ki67^{high}CD4^{+} T cells (D), carcinoma Ki67^{high}CD8^{+} T cells (E), and stromal Ki67^{high}CD8^{+} T cells (F). P values of the density and proportion were analyzed by the Steel test and Dunnett's test, respectively. G, Ratio of carcinoma to stromal Ki67^{high}CD4^{+} T cells (left graph) and Ki67^{high}CD8^{+} T cells (right graph). P values were analyzed by Dunnett's test. Cont., control; CRT, chemoradiotherapy; NAC, neoadjuvant chemotherapy

Ki67^{high} T cells, except for carcinoma Ki67^{high}CD8^{+} T cells, were comparable (Figure 3C–F). Both CRT and NAC groups showed notable differences in the carcinoma / stromal ratio of Ki67^{high} T-cell subsets; the ratio of Ki67^{high}CD4^{+} T cells was higher in the CRT group, whereas the ratio of Ki67^{high}CD8^{+} T cells was higher after NAC (Figure 3G).
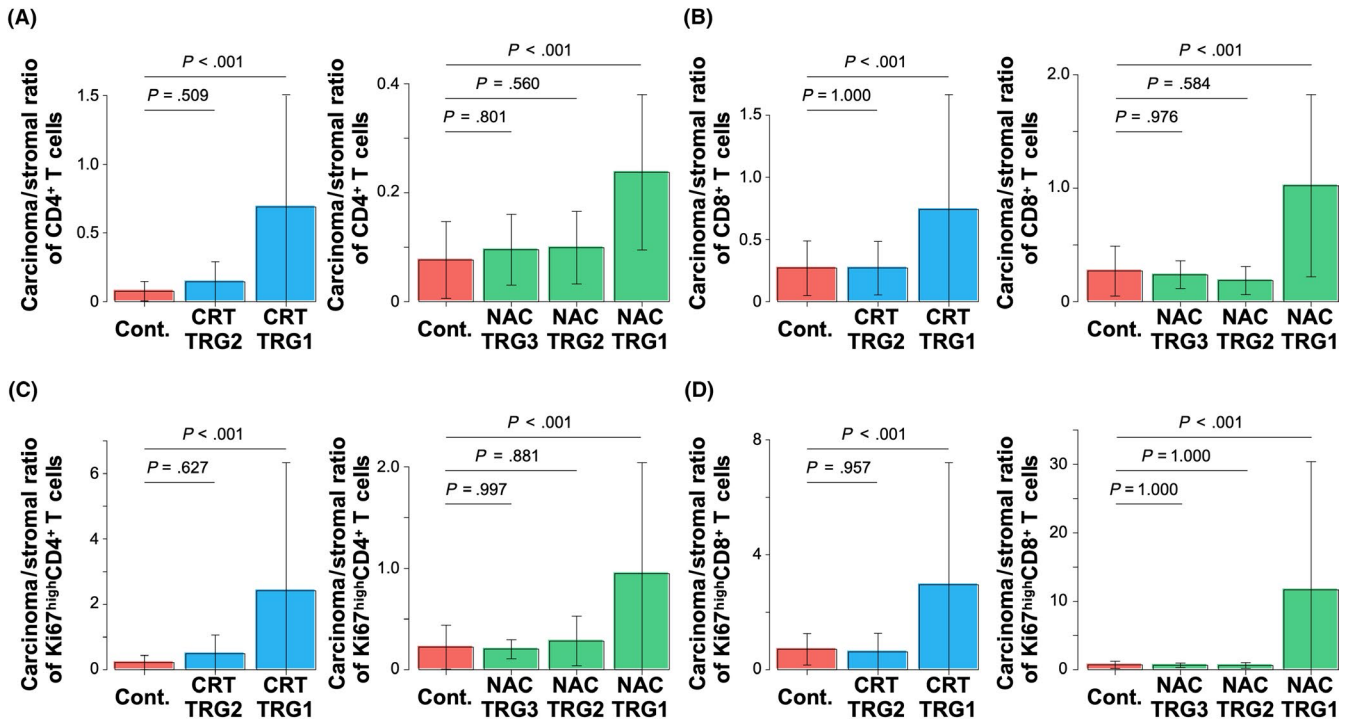
FIGURE 4 Infiltration of T-cell subsets depending on the local treatment effect after neoadjuvant therapies for rectal cancer. A–D, Evaluation between tumor regression grade (TRG) after chemoradiotherapy (CRT) (left graph) or neoadjuvant chemotherapy (NAC) (right graph) and ratio of carcinoma to stromal CD4$^+$ T cells (A), CD8$^+$ T cells (B), Ki67^{high}CD4$^+$ T cells (C), and Ki67^{high}CD8$^+$ T cells (D). P values were analyzed by Dunnett's test

3.5 | Correlation between T cell subsets and local treatment effect

Subsequently, to evaluate the role of T cell subsets on local treatment effects, we evaluated the correlation between T cell subset localization and TRG. The density of each T cell subset for each TRG patient is shown in Figure S4. After CRT, the densities of stromal T cells in all TRG patients were decreased, whereas the densities of carcinoma T cells in TRG1 patients were maintained. After NAC, the densities of carcinoma T cells tended to increase in all TRG patients; stromal T cells showed a similar increasing trend, with the exception of TRG1 patients. The carcinoma / stromal ratios showed more prominent results and were significantly higher in TRG1 patients after both neoadjuvant therapies than in the control group (Figure 4A, B). In particular, there was a marked increase in carcinoma / stromal ratios of Ki67^{high} subsets compared with that of total subsets (Figure 4C, D). Although CD4$^+$ and CD8$^+$ T cell density in the carcinoma or stromal areas showed different behaviors between CRT and NAC, T cells infiltrated the carcinoma area more readily after both neoadjuvant therapies, especially in patients who experienced significant tumor regression.

Because the Foxp3 transcriptional factor is well known as a marker of regulatory T cells (Tregs)—a subset of CD4$^+$ T cells that have a strong immunosuppressive function[34-37]— we examined the effects of CRT and NAC on Treg subsets by Foxp3 staining (Figure S5A). The proportion of Foxp3^{high} Tregs in the stromal CD4$^+$ T cell subset was decreased after neoadjuvant therapies (Figure S5B, C),

which was associated with the treatment effects (TRG) of both neoadjuvant therapies (Figure S5D). In contrast, the proportion of the Treg subset in carcinomas did not change among the 3 groups. We also analyzed the role of macrophages as immunosuppressive cells (Figure S6A, B). CD68$^+$ macrophages increased significantly after NAC and tended to increase after CRT (Figure S6C). Analysis of the CD68$^+$ population based on the M1 (CD68$^+$CD204$^-$) and M2 (CD68$^+$CD204$^+$) macrophage phenotypes revealed that M1 levels increased significantly after both CRT and NAC (Figure S6D).

3.6 | Contributions of Ki67^{high} T cells to RFS after neoadjuvant therapies

To assess the effects of T cell subsets on prognosis, we classified patients in the CRT and the NAC groups as high or low cases using the median of T cell densities and carcinoma / stromal ratios. Univariate Cox proportional hazards analysis indicated that the densities of both Ki67^{high}CD4$^+$ and CD8$^+$ T cells were associated with better prognosis; the high densities of carcinoma Ki67^{high}CD4$^+$ T cells after CRT and stromal Ki67^{high}CD8$^+$ T cells after NAC could significantly inhibit recurrence. The densities of CD4$^+$ and CD8$^+$ T cells in the CRT group and CD8$^+$ T cells in the NAC group tended to be associated with better prognoses, although the differences were not statistically significant. In contrast, there were no differences in the carcinoma / stromal ratios between the high and low cases (Table 2).

TABLE 2 Univariate analysis associated with T-cell subsets in patients with rectal cancer who received neoadjuvant chemoradiotherapy or chemotherapy

T-cell subset	CRT (n = 41)			NAC (n = 46)		
	HR	95% CI	*P* value	HR	95% CI	*P* value
Carcinoma CD4+ T cells (high/low)	0.497	0.192-1.285	.149	1.005	0.408-2.476	.991
Stromal CD4+ T cells (high/low)	0.914	0.362-2.306	.849	0.945	0.383-2.327	.901
Carcinoma CD8+ T cells (high/low)	0.389	0.146-1.038	.059	0.502	0.198-1.277	.148
Stromal CD8 T cells (high/low)	0.510	0.197-1.316	.164	0.484	0.190-1.231	.128
Carcinoma / stromal ratio of CD4+ T cells (high/low)	0.885	0.351-2.232	.796	1.102	0.448-2.716	.832
Carcinoma / stromal ratio of CD8+ T cells (high/low)	0.828	0.327-2.100	.691	1.044	0.424-2.570	.926
Carcinoma Ki67^{high}CD4+ T cells (high/low)	0.366	0.137-0.979	.045	0.747	0.300-1.860	.531
Stromal Ki67^{high}CD4+ T cells (high/low)	0.471	0.182-1.219	.121	0.739	0.297-1.839	.516
Carcinoma Ki67^{high}CD8+ T cells (high/low)	0.513	0.199-1.325	.168	0.492	0.194-1.253	.137
Stromal Ki67^{high}CD8+ T cells (high/low)	0.517	0.200-1.335	.173	0.377	0.143-0.994	.049
Carcinoma / stromal ratio of Ki67^{high}CD4+ T cells (high/low)	1.403	0.553-3.562	.476	1.172	0.476-2.888	.730
Carcinoma / stromal ratio of Ki67^{high}CD8+ T cells (high/low)	1.319	0.520-3.346	.560	1.154	0.469-2.842	.755

Abbreviations: CI, confidence interval; CRT, chemoradiotherapy; HR, hazard ratio; NAC, neoadjuvant chemotherapy.

Finally, we applied the univariate analysis and the following multivariate Cox proportional hazards analysis to assessing the importance of various covariates in pathological features and T cell subsets for RFS. We found that LYI as well as the densities of carcinoma Ki67^{high}CD4+ T cells after CRT and stromal Ki67^{high}CD8+ T cells after NAC were significantly independent predictive factors (Table 3). Kaplan-Meier analysis of RFS using the density of these T cell subsets in both the CRT and NAC groups is shown in Figure 5.

4 | DISCUSSION

In this study, we first assessed the effect of neoadjuvant therapies, CRT and NAC, on the tumor microenvironments of advanced RC. While CRT and NAC had different effects on the density of CD4+ and CD8+ T cells in tumor tissues, the aggressive migration of TILs into carcinomas was observed after both therapies. Notably, we found that T cell subsets with high expression of Ki67 —a T cell activation marker— were significantly correlated with good prognosis after neoadjuvant therapies. Our results indicate the clinical significance of T cell activation and its localization in RC after neoadjuvant therapies.

Using CK staining and computational evaluation of the carcinoma area, we confirmed the effect of neoadjuvant therapies on residual carcinomas. Regarding the morphology, CRT led to disruption of the carcinoma masses, whereas NAC induced its shrinkage. Based on an analysis of Ki67 expression, residual carcinoma masses had a

higher proliferative capacity in the NAC group than in the CRT group. Previous reports have shown that, compared with NAC, CRT controls local tumors more effectively,[38,39] which is consistent with our results. These differences in therapeutic outcomes could be attributed to mechanisms during NAC, wherein chemotherapeutic agents reach the tumor by way of the marginal tissue through abundant blood flow, leading to shrinkage of the carcinoma mass over time. However, NAC cannot control regrowth of the residual carcinoma masses after a drug has penetrated the tumor tissues. In contrast, irradiation directly damages not only the carcinoma but also the normal tissue around it, including the tumor stroma, by inducing apoptosis, disrupting whole tumor tissues, and causing fibrosis.[40] Additionally, cumulative DNA damage in residual carcinoma cells, resulting from fractionated irradiation, causes longer growth suppression of carcinoma cells.

After evaluating lymphocyte infiltration, we found an increased density of TILs after NAC of RC. Similarly, Tsuchikawa et al[41] reported that the CD4+ and CD8+ cell count is increased after neoadjuvant chemotherapy of esophageal squamous cell carcinoma. Chemotherapy induces the accumulation of CD4+ cells in tumors via inflammatory responses and is accompanied by an upregulation of chemokines.[42] However, this study and our previous reports found that the T cell density in tumor tissues decreased after CRT.[43] Conversely, Shinto et al[15] reported that the number of stromal CD8+ cells in RC increased after neoadjuvant CRT. These discrepancies in immunological observations after CRT might be due to the radiation dose and interval time between the last irradiation to resection; in

TABLE 3 Univariate and multivariate analyses associated with pathological features and T-cell subsets in patients with rectal cancer who received neoadjuvant chemoradiotherapy or chemotherapy

Factor	CRT (n = 41)					NAC (n = 46)				
		Univariate analysis		Multivariate analysis			Univariate analysis		Multivariate analysis	
	n	HR (95% CI)	P value	HR (95% CI)	P value	n	HR (95% CI)	P value	HR (95% CI)	P value
Pathological TNM stage										
I	10	0.307 (0.071-1.339)	.116	—		13	0.109 (0.015-0.817)	.031	0.259 (0.031-2.173)	.213
II/III	31	Ref		Ref		33	Ref		Ref	
Lymphatic invasion										
Present	10	3.076 (1.176-8.046)	.022	3.401 (1.183-9.780)	.023	22	2.251 (0.886-5.720)	.088	—	
Absent	31	Ref		Ref		24	Ref			
Vascular invasion										
Present	24	0.829 (0.327-2.100)	.692	—		21	4.532 (1.628-12.62)	.004	2.619 (0.754-9.099)	.130
Absent	17	Ref				25	Ref		Ref	
Perineural invasion										
Present	14	2.548 (1.009-6.435)	.048	1.978 (0.756-5.174)	.164	12	3.646 (1.469-9.045)	.005	2.274 (0.707-7.317)	.168
Absent	27	Ref		Ref		34	Ref		Ref	
Tumor regression grade										
1	17	0.597 (0.224-1.595)	.304	—		13	0.809 (0.291-2.248)	.685	—	
2/3	24	Ref				33	Ref			
Carcinoma $Ki67^{high}$CD4$^+$ T cells										
High	21	0.366 (0.137-0.979)	.045	0.270 (0.094-0.777)	.015	23	0.747 (0.300-1.860)	.531	—	
Low	20	Ref		Ref		23	Ref			
Stromal $Ki67^{high}$CD8$^+$ T cells										
High	21	0.517 (0.200-1.335)	.173	—		23	0.377 (0.143-0.994)	.049	0.274 (0.094-0.799)	.018
Low	20	Ref				23	Ref		Ref	

Abbreviations: —, not applicable; CI, confidence interval; CRT, chemoradiotherapy; HR, hazard ratio; NAC, neoadjuvant chemotherapy; Ref, reference.
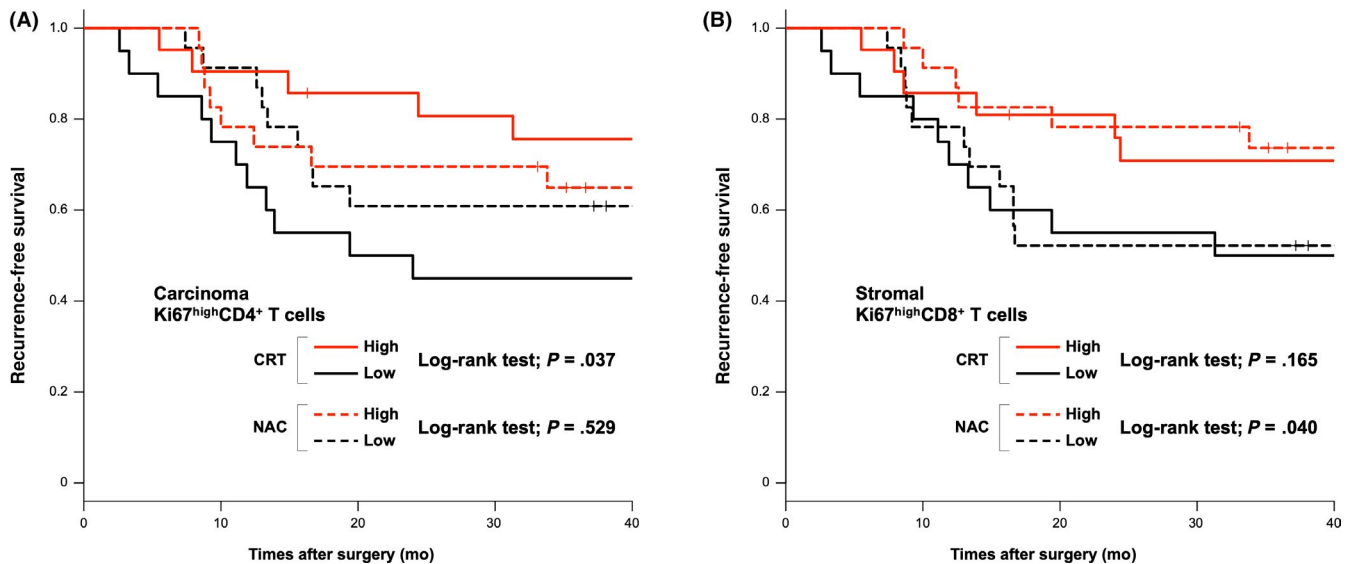
FIGURE 5 Kaplan-Meier curves of recurrence-free survival (RFS) after neoadjuvant therapies for rectal cancer according to the densities of Ki67^{high} T-cell subsets. A, B, According to the densities of carcinoma Ki67^{high}CD4$^+$ T cells (A) or Ki67^{high}CD8$^+$ T cells (B), patients were classified into high or low groups based on the median value. RFS of patients who received chemoradiotherapy (CRT) or neoadjuvant chemotherapy (NAC) are shown as bold lines and dotted lines, respectively. The color range indicates the accumulation of lymphocytes, with high accumulation shown in red and low accumulation shown in black. P values were analyzed by a log-rank test

the present study, surgical resection was carried out 4-12 weeks after neoadjuvant CRT at 45 to 50.4 Gy, whereas, for Shinto et al,[15] resection was carried out 4 weeks after irradiation with 20 Gy. Long-term fractionated irradiation on local tumors results in transient lymphopenia in tumor tissues, accompanied by tumor regression. Moreover, our results of increased T cells in cancer tissues after NAC could support a combination therapy with immunological checkpoint blockade for RC. Our findings highlight the importance of combination therapies with radiotherapy and cancer immunotherapy; short-term fractionated irradiation and longer interval times could be optimal for the preservation of immunological surveillance against cancer.

Despite the different effects of the neoadjuvant therapies on T cell density, both therapies induced the aggressive infiltration of TILs into carcinoma masses, accompanied by tumor regression. However, no significant correlation was observed between the carcinoma / stromal ratio of T cells and patient RFS. This finding indicates that there are different mechanisms between the antitumor immune response against the local tumor and the immune surveillance associated with suppression of systemic recurrence. Similar to a previous report regarding the effect of neoadjuvant therapies on antitumor immunity in other cancer types,[44] our finding suggests that the antitumor immune response can be enhanced during neoadjuvant therapies of advanced RC via antigen spreading and the initiation of danger signals. Moreover, as baseline tumor size could be an independent prediction marker for the efficacy of immune checkpoint inhibitors,[45] the combination of immune checkpoint inhibitors and neoadjuvant therapies for partial tumor reduction could be effective for RC treatment.

We further found that the correlation between important TIL subsets and their localization with prognosis differed between the CRT and NAC groups. For CRT, both Ki67^{high}CD4$^+$ and Ki67^{high}CD8$^+$ T cell density contributed to suppress systemic recurrence; in particular, an

increased density of Ki67^{high}CD4$^+$ T cells in the carcinoma area significantly prolonged RFS. Meanwhile, stromal Ki67^{high}CD8$^+$ T cells after NAC mostly contributed to prolong RFS. Although the CD4$^+$ population significantly increased after NAC, this population was not associated with improved RFS. These results suggest that different neoadjuvant therapies initiated immune surveillance against the tumors by different mechanisms; the helper function of CD4$^+$ T cells is important after CRT, but not after NAC. The enhancement of cytotoxic T lymphocyte (CTL) activity by CRT (abscopal effect) was reported to require the function of helper CD4$^+$ T cells through the activation of tumor-infiltrating antigen-presenting cells (APCs), such as tumor-associated macrophages and dendritic cells.[46,47] However, the activation of APCs after NAC would be induced nonspecifically without the help of CD4$^+$ T cells because a robust infiltration of T cells accompanied by the inflammatory response was observed in the local tumor site.[42] Therefore, enhancement of CTL activity could occur independently of CD4$^+$ T cell activation during NAC.

Regarding the role of the immunosuppressive population, we found that the proportion of carcinoma Tregs did not change among the 3 groups, whereas stromal Tregs were significantly decreased and accompanied by tumor regression. The Treg density after NAC increased, but this was associated with the increase in total CD4$^+$ T cells. These findings suggest that the selective depletion of stromal Tregs by neoadjuvant therapies leads to the infiltration of activated CTL, followed by local tumor elimination. After analyzing tumor-infiltrating macrophages, we found that both neoadjuvant therapies increased polarization towards M1 macrophages, which have been reported to robustly express MHC class II.[48] Thus, we theorized that both CRT and NAC can polarize tumor-infiltrating macrophages, resulting in improvement of the tumor immune environment, which is similar to the depletion of stromal Tregs. Although neoadjuvant therapies could improve the local tumor immune environment, they did not contribute to the prolongation of RFS

(Table S2). We found that lower densities of Ki67^highCD4+ and CD8+ T cells tended to correlate with a lower infiltration of Tregs (data not shown), resulting in a shorter RFS. Further experiments are warranted to uncover the role of CD4+ T cells in the antitumor immune response during neoadjuvant therapies, especially NAC.

In summary, we found that the evaluation of activated T cells expressing Ki67 and their localization in tumors is a reliable immunological marker for predicting the prognosis of locally advanced RC patients who received neoadjuvant therapy. Our results were also confirmed and practically validated by H&E staining and immunohistochemistry double staining (Figure S7). Previously, accumulation of mononuclear cells around the carcinoma nest observed by H&E staining was reported as a predictor of favorable prognosis.[49] This is in agreement with our findings on immunological features identified by mFIHC, which were associated with patient prognosis. There are some limitations to our study, however. It has been reported that MMR status could provide important information, eg, dMMR shows increased tumor mutation burden associated with high T cell infiltration.[50] However, in our study, we could not find any significant difference in the TILs between dMMR and proficient MMR across all groups (data not shown). We believe that the small population of dMMR in all groups was why dMMR status had less impact on TIL status. Moreover, this is a retrospective study that only used resected tumor tissues from a patient cohort enrolled in our hospital. There were no data on TILs before neoadjuvant therapies. In addition, although the median value was used as a threshold for separation of patients presenting with a high or low accumulation of lymphocytes, the threshold of T cells expressing Ki67 associated with prognosis has not been adequately studied. Therefore, a prospective study to assess postoperative prognosis following neoadjuvant therapies is warranted. Nevertheless, our findings can provide important insights for determining advanced RC prognosis after neoadjuvant therapies.

DISCLOSURE

The authors report no conflict of interest.

ORCID

Ken Imaizumi   https://orcid.org/0000-0002-7751-6270
Toshihiro Suzuki   https://orcid.org/0000-0002-7095-6556
Motohiro Kojima   https://orcid.org/0000-0002-6150-6545
Naoki Sakuyama   https://orcid.org/0000-0003-2711-1168
Tetsuya Nakatsura   https://orcid.org/0000-0003-3918-2385

REFERENCES

1. Bullard KM, Trudel JL, Baxter NN, et al. Primary perineal wound closure after preoperative radiotherapy and abdominoperineal resection has a high incidence of wound failure. *Dis Colon Rectum.* 2005;48:438-443.
2. Imaizumi K, Nishizawa Y, Ikeda K, et al. Extended pelvic resection for rectal and anal canal tumors is a significant risk factor for perineal wound infection: a retrospective cohort study. *Surg Today.* 2018;48:978-985.
3. Ito M, Saito N, Sugito M, et al. Analysis of clinical factors associated with anal function after intersphincteric resection for very low rectal cancer. *Dis Colon Rectum.* 2009;52:64-70.
4. Nishizawa Y, Fujii S, Saito N, et al. The association between anal function and neural degeneration after preoperative chemoradiotherapy followed by intersphincteric resection. *Dis Colon Rectum.* 2011;54:1423-1429.
5. Schrag D, Weiser MR, Goodman KA, et al. Neoadjuvant chemotherapy without routine use of radiation therapy for patients with locally advanced rectal cancer: A pilot trial. *J Clin Oncol.* 2014;32:513-518.
6. Deng Y, Chi P, Lan P, et al. Modified FOLFOX6 with or without radiation versus fluorouracil and leucovorin with radiation in neoadjuvant treatment of locally advanced rectal cancer: Initial results of the Chinese FOWARC multicenter, open-label, randomized three-arm phase III trial. *J Clin Oncol.* 2016;34:3300-3307.
7. Rouanet P, Rullier E, Lelong B, et al. Tailored treatment strategy for locally advanced rectal carcinoma based on the tumor response to induction chemotherapy. *Dis Colon Rectum.* 2017;60: 653-663.
8. McDonnell AM, Nowak AK, Lake RA. Contribution of the immune system to the chemotherapeutic response. *Semin Immunopathol.* 2011;33:353-367.
9. Zitvogel L, Galluzzi L, Smyth MJ, et al. Mechanism of action of conventional and targeted anticancer therapies: reinstating immunosurveillance. *Immunity.* 2013;39:74-88.
10. Cho Y, Miyamoto M, Kato K, et al. CD4+ and CD8+ T cells cooperate to improve prognosis of patients with Esophageal squamous cell carcinoma. *Cancer Res.* 2003;63(1555–1559):11.
11. Zhang L, Conejo-Garcia JR, Katsaros D, et al. Intratumoral T cells, recurrence, and survival in epithelial ovarian cancer. *N Engl J Med.* 2003;348:203-213.
12. Hiraoka K, Miyamoto M, Cho Y, et al. Concurrent infiltration by CD8+ T cells and CD4+ T cells is a favourable prognostic factor in non-small-cell lung carcinoma. *Br J Cancer.* 2006;94:275-280.
13. Loi S, Sirtaine N, Piette F, et al. Prognostic and predictive value of tumor-infiltrating lymphocytes in a phase III randomized adjuvant breast cancer trial in node-positive breast cancer comparing the addition of docetaxel to doxorubicin with doxorubicin-based chemotherapy: BIG 02–98. *J Clin Oncol.* 2013;31:860-867.
14. Anitei MG, Zeitoun G, Mlecnik B, et al. Prognostic and predictive values of the immunoscore in patients with rectal cancer. *Clin Cancer Res.* 2014;20:1891-1899.
15. Shinto E, Hase K, Hashiguchi Y, et al. CD8+ and FOXP3+ tumor-infiltrating T cells before and after chemoradiotherapy for rectal cancer. *Ann Surg Oncol.* 2014;21:414-421.
16. Yi JS, Ready N, Healy P, et al. Immune activation in early stage non-small cell lung cancer patients receiving neoadjuvant chemotherapy plus ipilimumab. *Clin Cancer Res.* 2017;23:7474-7482.
17. Rutkowski P, Kozak K. News from the melanoma sessions of the European Cancer Congress 2017. *BMC Med.* 2017;15:57.
18. Forde PM, Smith KN, Chaft JE, et al. stage Neoadjuvant anti-PD1, nivolumab, in early stage resectable non-small-cell lung cancer. *Ann Oncol.* 2016;27:vi552–vi587.
19. Le DT, Uram JN, Wang H, et al. PD-1 blockade in tumors with mismatch-repair deficiency. *N Engl J Med.* 2015;372:2509-2520.

20. Cross M. ERG oncoprotein overexpression in prostate cancer. Multiplex IHC adds to diagnostic prowess and efficiency of laboratory. *MLO Med Lab Obs*. 2011;43:22-42.

21. Stack EC, Wang C, Roman KA, et al. Multiplexed immunohistochemistry, imaging, and quantitation: a review, with an assessment of Tyramide signal amplification, multispectral imaging and multiplex analysis. *Methods*. 2014;70:46-58.

22. Feng Z, Puri S, Moudgil T, et al. Multispectral imaging of formalin-fixed tissue predicts ability to generate tumor- infiltrating lymphocytes from melanoma. *J Immunother Cancer*. 2015;3:47.

23. Mlecnik B, Bindea G, Angell HK, et al. Integrative analyses of colorectal cancer show immunoscore is a stronger predictor of patient survival than microsatellite instability. *Immunity*. 2016;44:698-711.

24. Igari F, Horimoto Y, Takahashi Y, et al. Diagnostic significance of intratumoral CD8+ tumor infiltrating lymphocytes in medullary carcinoma. *Hum Pathol*. 2017;70:129-138.

25. Tumeh PC, Harview CL, Yearley JH, et al. PD-1 blockade induces responses by inhibiting adaptive immune resistance. *Nature*. 2014;515:568-571.

26. Hazenberg MD, Stuart JW, Otto SA, et al. T-cell division in human immunodeficiency virus (HIV)-1 infection is mainly due to immune activation: a longitudinal analysis in patients before and during highly active antiretroviral therapy (HAART). *Blood*. 2000;95:249-255.

27. Papagno L, Spina CA, Marchant A, et al. Immune activation and CD8+ T-cell differentiation towards senescence in HIV-1 infection. *PLoS Biol*. 2004;2:E20.

28. Edge SB, Compton CC. The American Joint Committee on Cancer: the 7th edition of the AJCC cancer staging manual and the future of TNM. *Ann Surg Oncol*. 2010;17:1471-1474.

29. Mace AG, Pai RK, Stocchi L, et al. American joint committee on cancer and College of American pathologists regression grade: a new prognostic factor in rectal cancer. *Dis Colon Rectum*. 2015;58:32-44.

30. Shinto E, Tsuda H, Ueno H, et al. Prognostic implication of laminin-5 gamma 2 chain expression in the invasive front of colorectal cancers, disclosed by area-specific four-point tissue microarrays. *Lab Invest*. 2004;85:257-266.

31. Kojima M, Higuchi Y, Yokota M, et al. Human subperitoneal fibroblast and cancer cell interaction creates microenvironment that enhances tumor progression and metastasis. *PLoS ONE*. 2014;9:e88018.

32. Takahashi D, Kojima M, Suzuki T, et al. Profiling the tumour immune microenvironment in pancreatic neuroendocrine neoplasms with multispectral imaging indicates distinct subpopulation characteristics concordant with WHO 2017 classification. *Sci Rep*. 2018;8:13166.

33. Kanda Y. Investigation of the freely available easy-to-use software "EZR" for medical statistics. *Bone Marrow Transplant*. 2013;48:452-458.

34. Curiel TJ, Coukos G, Zou L, et al. Specific recruitment of regulatory T cells in ovarian carcinoma fosters immune privilege and predicts reduced survival. *Nat Med*. 2004;10:942-949.

35. Bates GJ, Fox SB, Han C, et al. Quantification of regulatory T cells enables the identification of high-risk breast cancer patients and those at risk of late relapse. *J Clin Oncol*. 2006;24:5373-5380.

36. Mougiakakos D, Johansson CC, Trocme E, et al. Intratumoral forkhead box P3-positive regulatory T cells predict poor survival in cyclooxygenase-2-positive uveal melanoma. *Cancer*. 2010;116:2224-2233.

37. Shimizu K, Nakata M, Hirami Y, et al. Tumor-infiltrating Foxp3+ regulatory T cells are correlated with cyclooxygenase-2 expression and are associated with recurrence in resected non-small cell lung cancer. *J Thorac Oncol*. 2010;5:585-590.

38. Peeters KCMJ, Marijnen CAM, Nagtegaal ID, et al. The TME trial after a median follow-up of 6 years: Increased local control but no survival benefit in irradiated patients with resectable rectal carcinoma. *Ann Surg*. 2007;246:693-701.

39. Sakuyama N, Kojima M, Kawano S, et al. Area of residual tumor is a robust prognostic marker for patients with rectal cancer undergoing preoperative therapy. *Cancer Sci*. 2018;109:871-878.

40. Kelley ST, Coppola D, Yeatman T, et al. Tumor response to neoadjuvant chemoradiation therapy for rectal adenocarcinoma is mediated by p53-dependent and caspase 8-dependent apoptotic pathways. *Clin Colorectal Cancer*. 2005;5:114-118.

41. Tsuchikawa T, Yamamura Y, Shichinohe T, et al. The immunological impact of neoadjuvant chemotherapy on the tumor microenvironment of esophageal squamous cell carcinoma. *Ann Surg Oncol*. 2012;19:1713-1719.

42. Denkert C, Loibl S, Noske A, et al. Tumor-associated lymphocytes as an independent predictor of response to neoadjuvant chemotherapy in breast cancer. *J Clin Oncol*. 2010;28:105-113.

43. Sakuyama N, Kojima M, Kawano S, et al. Histological differences between preoperative chemoradiotherapy and chemotherapy for rectal cancer: a clinicopathological study. *Pathol Int*. 2016;66:273-280.

44. Gulley JL, Madan RA, Pachynski R, et al. Role of antigen spread and distinctive characteristics of immunotherapy in cancer treatment. *J Natl Cancer Inst*. 2017;109(4);https://doi.org/10.1093/jnci/djw261

45. Joseph RW, Elassaiss-Schaap J, Kefford R, et al. Baseline tumor size is an independent prognostic factor for overall survival in patients with melanoma treated with pembrolizumab. *Clin Cancer Res*. 2018;24:4960-4967.

46. Kono K, Mimura K, Kiessling R. Immunogenic tumor cell death induced by chemoradiotherapy: molecular mechanisms and a clinical translation. *Cell Death Dis*. 2013;4:e688-e696.

47. Kubo M, Satoh T, Ishiyama H, et al. Enhanced activated T cell subsets in prostate cancer patients receiving iodine-125 low-dose-rate prostate brachytherapy. *Oncol Rep*. 2017;39:417-424.

48. Wijesundera KK, Izawa T, Tennakoon AH, et al. M1- and M2-macrophage polarization in rat liver cirrhosis induced by thioacetamide (TAA), focusing on Iba1 and galectin-3. *Exp Mol Pathol*. 2014;96:382-392.

49. Shia J, Guillem JG, Moore HG, et al. Patterns of morphologic alteration in residual rectal carcinoma following preoperative chemoradiation and their association with long-term outcome. *Am J Surg Pathol*. 2004;28:215-223.

50. Laghi L, Bianchi P, Miranda E, et al. CD3+ cells at the invasive margin of deeply invading (pT3-T4) colorectal cancer and risk of post-surgical metastasis: a longitudinal study. *Lancet Oncol*. 2009;10:877-884.

SUPPORTING INFORMATION

Additional supporting information may be found online in the Supporting Information section.